

# A Study on Effect of Section Thickness in Friction Stir Welding of Ferritic-Martensitic Steel

Vijaya Lakshmi Manugula

Department of Metallurgical and Materials Engineering,  
Mahatma Gandhi Institute of Technology,  
Hyderabad 500 075

**Abstract:-** Friction Stir Welding (FSW) has been conducted on 6 mm and 12 mm thickness plates of a Reduced Activation Ferritic-Martensitic Steel using polycrystalline cubic boron nitride tool with a view of understanding section thickness and tool rotational speed effects on evolving microstructure in various zones and hardness across the weld joint. The FSW joint was composed of stir zone (SZ), thermo mechanical affected zone (TMAZ), heat affected zone (HAZ) and base metal (BM). The BM microstructure comprises of tempered lath martensite with prior austenite grain boundaries and lath boundaries decorated with chromium rich  $M_{23}C_6$  type carbides and very fine tantalum or vanadium rich MX type carbides in the intra lath regions. During FSW BM microstructure was altered based on the rotational speed of the tool and section thickness of the plate. The extent of various zones developed were found to have relation with section thickness. Rotational speeds at and above 300 rpm led to the occurrence of martensite in SZ. Irrespective of rotational speeds employed, the grain boundaries in the SZs have been found free from grain boundary carbides. The post weld heat treatment produced tempered martensite re-precipitated grain boundary carbides and leading to significant reduction in overall hardness in SZ. Pronounced reduction in hardness was also observed in the HAZ of 12 mm thick plate welds. It has been observed that the increase in section thickness has a great influence on the heat input required during FSW and on the resulting microstructure and hardness in the constituent zones of FSW joint.

**Keywords:** *Reduced Activation Ferritic - Martensitic steel, Friction Stir Welding, Post Weld Heat Treatment, Section Thickness, Heat Input*

## 1. INTRODUCTION

Indian Reduced Activation Ferritic-Martensitic (RAFM) steel has been developed as a structural material for fabrication of Test Blanket Module to be used in International Thermonuclear Experimental Reactor[1]. Fabrication of TBM calls for the development of suitable welding technologies. In general, fusion welding processes have been reported to cause the occurrence of delta-ferrite in the welds, which promotes the raise in ductile-to-brittle transition temperature and poor impact toughness[2-4]. This phase may also get transformed to a brittle sigma phase on long term exposure to elevated temperatures. Since FSW being a solid state welding process, it does not create molten metal in the weld and hence the problems associated with the conventional fusion welding processes could be minimised.

Very recently, several efforts have been directed on RAFM steels (F82H, EUROFER and INRAFM) towards assessing the effects of tool rotational and traverse speeds on evolving

microstructures and mechanical properties of various zones[5-9]. It has been shown that the increase in tool rotational speed increases the heat input and also lead to wider SZ and TMAZ; and post weld heat treatments are absolutely essential to bring down the high hardness developed in these zones due to martensite formation and improve the impact toughness of welded joints on par with the starting base material. Invariably, many of these studies were conducted on thin section material employing either PcBN or other refractory tool materials. Although thin sections may find application, majority of the components in TBM will likely be thicker in design. Additionally, severe thermal gradients during welding would likely lead to wider SZ, TMAZ and HAZ in thick sections; the effects of these on microstructure and mechanical properties is yet unknown. This paper reports the interesting results obtained on FSW of 6 and 12 mm thick INRAFM plates with respect to evolving microstructure and hardness variation across the weld joint. The effects of post weld heat treatment (PWHT) were also assessed on resulting microstructure and mechanical properties.

## 2. EXPERIMENTAL

Full penetration bead-on-plate FSW was conducted on 6 and 12mm thick plates, using conical threaded-pin PCBN tools with pin heights of 6 and 12 mm. The tools were tilted by 2 degrees from plate normal. Argon gas shielding was employed to prevent the oxidation of the surface during welding. The austenite transformation start ( $A_{c1}$ ) and finish ( $A_{c3}$ ) temperatures of this steel are 835°C and 875°C respectively [8]. The as-received material was in normalised (1253K/30 min /air cool) and tempered (1033K/60 min/air cool) condition. The chemical composition of this steel is given in Table.1. The FSW experimental conditions are summarised in Table.2. The welded samples were subjected to PWHT of 760°C/90 min/air cool to study the effect of PWHT on microstructure and mechanical properties. The optical microscopy and FEG-SEM were conducted on samples taken from different locations and etched with Villella's reagent (100ml ethanol, 5ml HCL, and 1 g picric acid). Vickers micro hardness test was performed on the mid plane of transverse cross section across the FSW joint. Load of 300g and dwell time of 20sec were used on indentations taken at regular intervals of 0.5mm.

### 3. RESULTS AND DISCUSSION

#### 3.1 Base metal microstructure

The base metal in normalised and tempered condition displayed fully tempered lath martensite (Fig.1). The prior austenite grain boundaries and lath boundaries were decorated with chromium rich  $M_{23}C_6$  type precipitates while the intra lath regions consisted of very fine MX type carbides/ carbo nitrides rich in V or Ta. During high temperature service, carbides on grain boundaries prevent grain boundary sliding, while carbides on lath boundaries restrict the coarsening of laths; both these factors are considered beneficial for high temperature creep strength.

#### 3.2 As welded condition

The macrostructure of the FSW joint is composed of stir zone, thermo mechanically affected zone (TMAZ), HAZ and base metal. Rotational speed exerted major influence on the width of SZ, TMAZ and HAZ developed, as shown in Fig.2 for 6mm thick plate. The higher rotational speed led to widening of TMAZ and SZ. The Vickers hardness profiles on transverse cross section in the mid thickness regime for the four rotational speeds are given in Fig. 3 . The hardness variation across the weld can be rationalised on the basis of prevailing microstructure in different zones. During FSW, the starting BM microstructure was altered in SZ both by heat and plastic deformation and entirely fresh microstructure emerged. The

Table.1 Chemical composition of Indian Reduced Activation Ferritic-Martensitic (INRAFM) steel.

|          |        |         |       |        |             |       |        |
|----------|--------|---------|-------|--------|-------------|-------|--------|
| elements | C      | W       | Mn    | Cr     | Ni          | S     | P      |
| Wt%      | 0.1    | 1.34    | 0.54  | 8.97   | 0.008       | 0.002 | 0.004  |
| elements | Ta     | B       | Al    | Cu     | O2          | N2    | Nb     |
| Wt%      | 0.066  | <0.0001 | 0.008 | <0.002 | 0.008       | 0.031 | <0.001 |
| elements | Mo     | Ti      | Co    | V      | As+Sn+Sb+Zr | Fe    | Si     |
| Wt%      | <0.002 | <0.005  | 0.007 | 0.23   | <0.03       | Bal   | 0.05   |

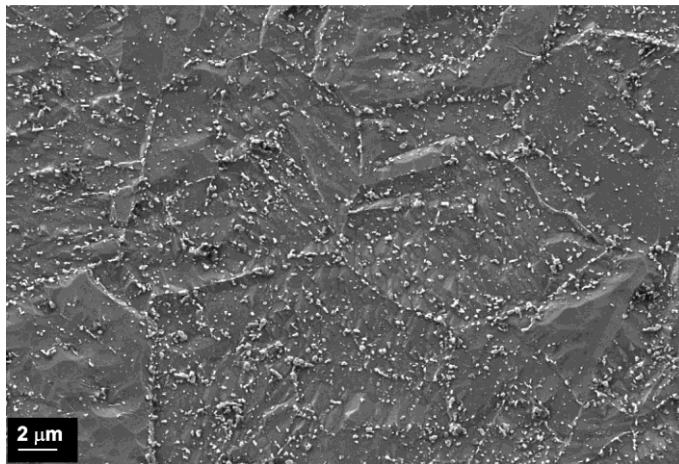


Fig.1 FE-SEM microstructure of Base metal in normalised and tempered condition showing prior austenite grain boundaries and lath boundaries decorated with chromium rich carbides.

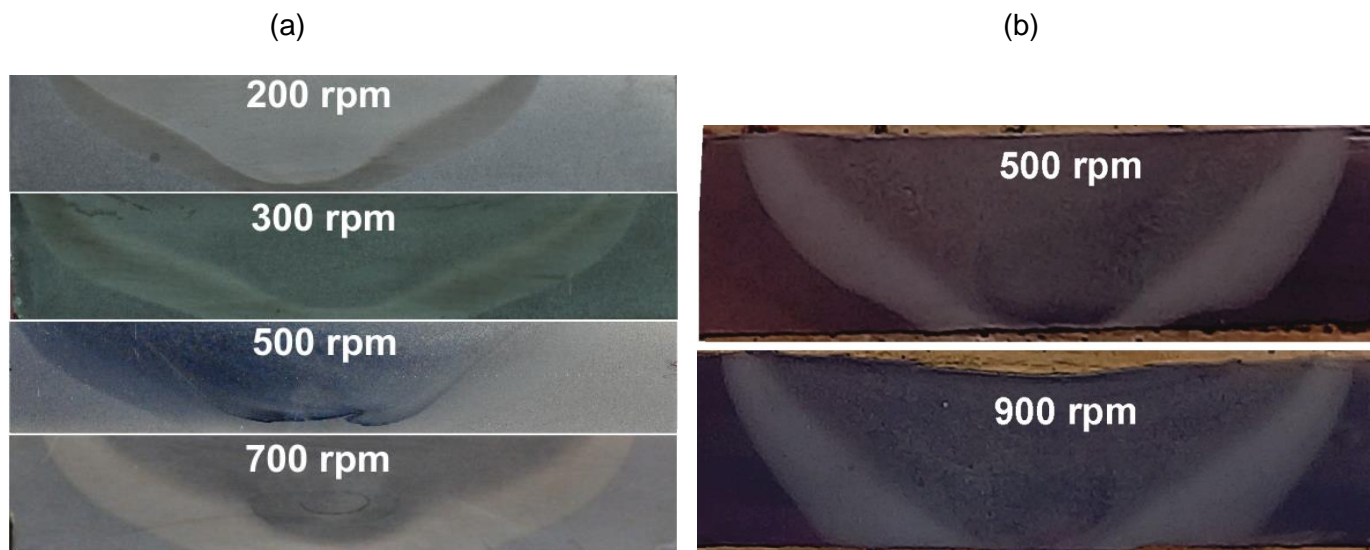


Fig.2. Macrostructure of cross-section of friction stir welds at various rotational speeds (a) 6mm (b) 12 mm.

Table.2 Welding parameters used in Friction stir welding of 6 and 12 mm thicknesses and heat input

| Case No | Material         | Rotational speed (RPM) | Travel speed (mm min <sup>-1</sup> ) | Heat input (kJ/mm) |
|---------|------------------|------------------------|--------------------------------------|--------------------|
| 1       | 6mm RAFM steel   | 200                    | 30                                   | 4.5                |
| 2       | 6mm RAFM steel   | 300                    | 30                                   | 5.27               |
| 3       | 6mm RAFM steel   | 500                    | 30                                   | 5.02               |
| 4       | 6mm RAFM steel   | 700                    | 30                                   | 5.27               |
| 5       | 12 mm RAFM steel | 500                    | 20                                   | 11.49              |
| 6       | 12 mm RAFM steel | 900                    | 20                                   | 12.71              |

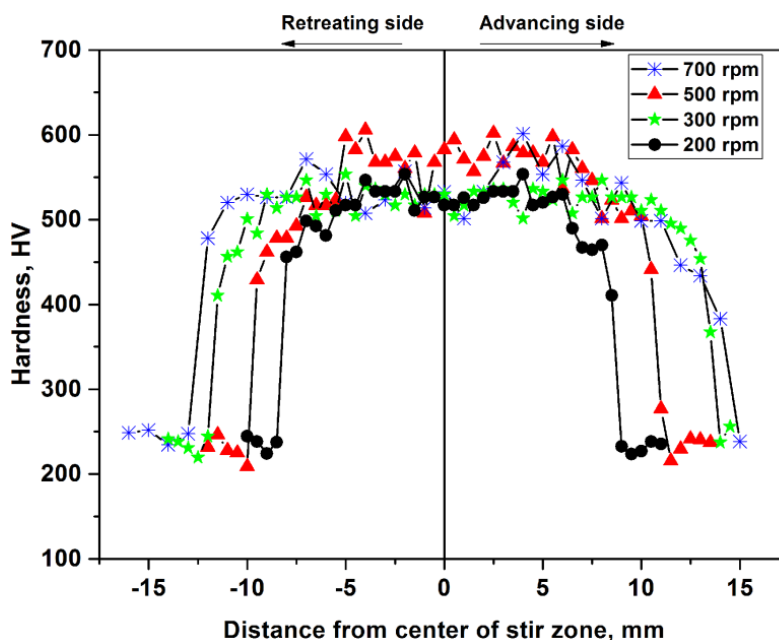


Fig .3 Vickers hardness profile in transverse section at mid plane at various rotational speeds for 6 mm thick plate



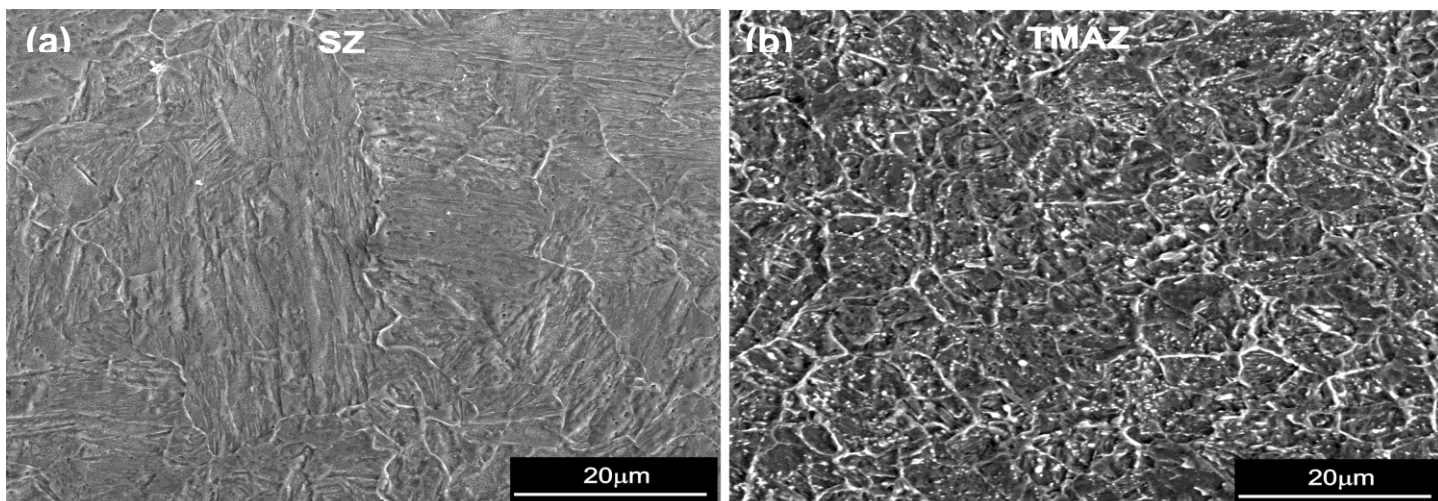


Fig..Fig.4.FE-SEM microstructures of SZ and TMAZ in as welded condition for 6 mm thick plate at 500rpm.

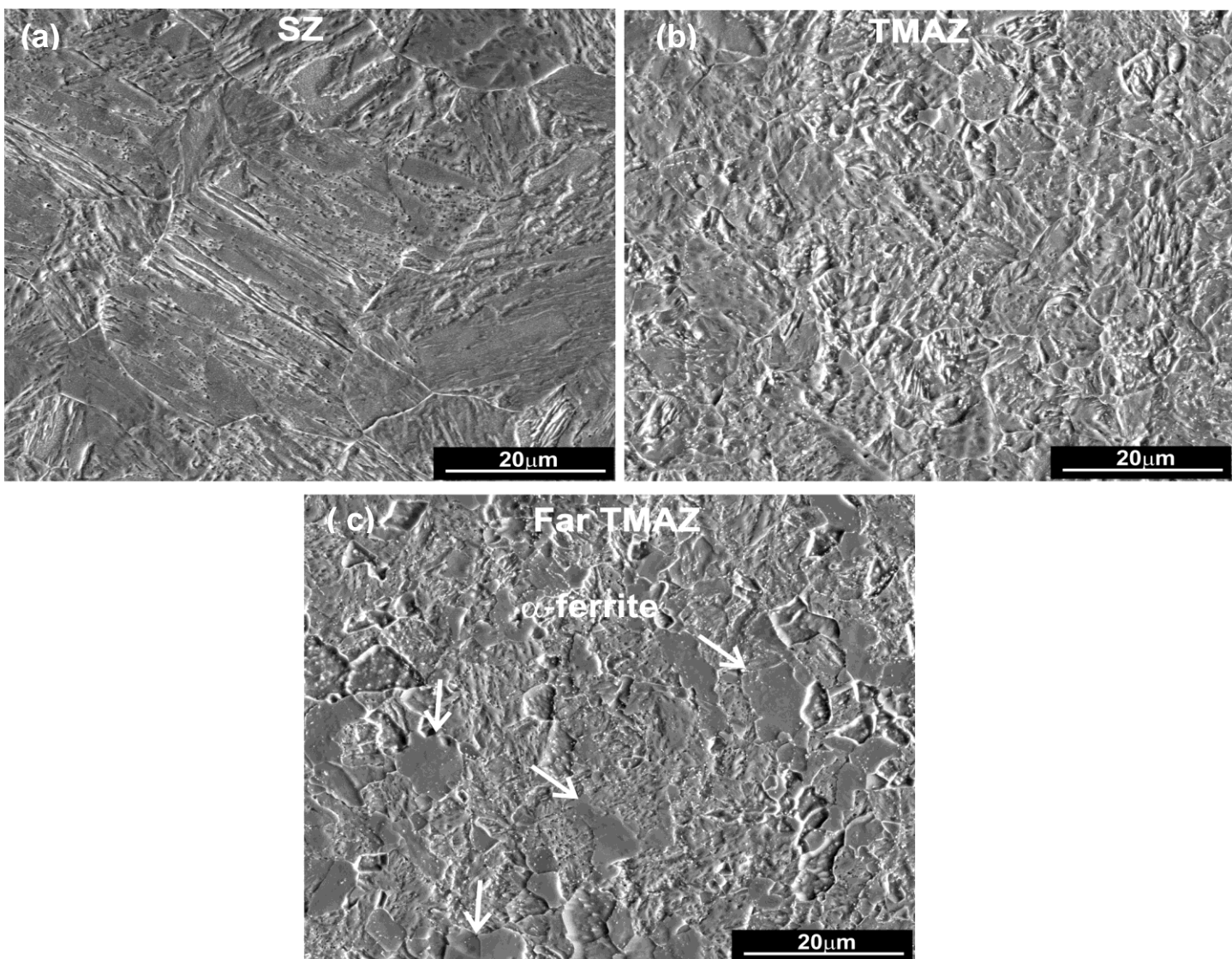


Fig..FFig.5 FE-SEM microstructures of SZ, TMAZ and far TMAZ in as welded condition for 12 mm thick at 500 rpm



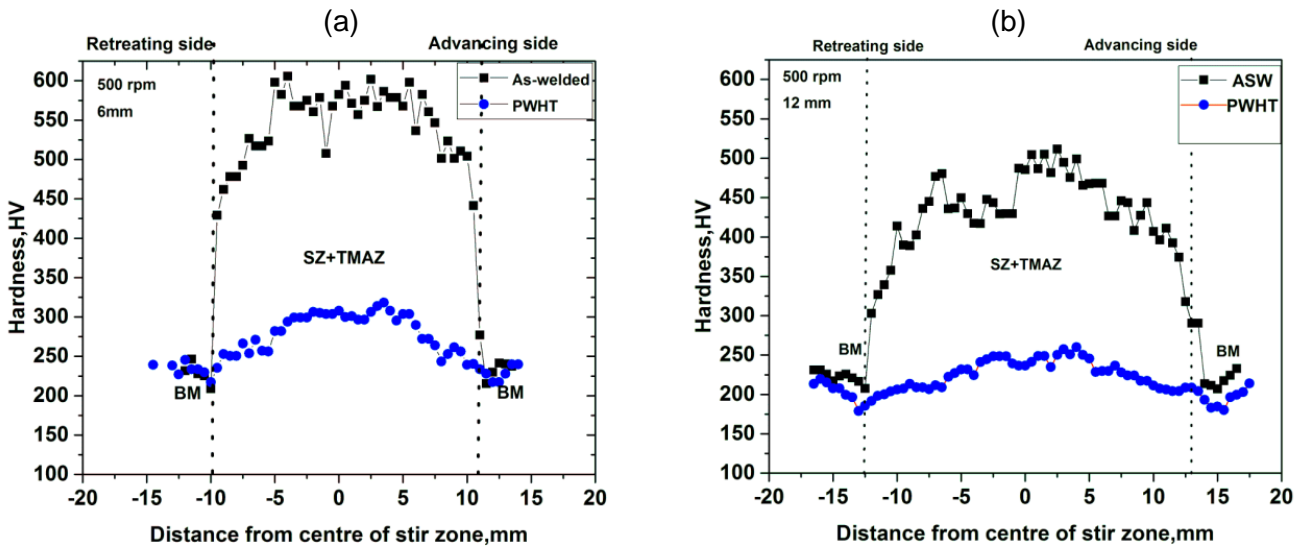
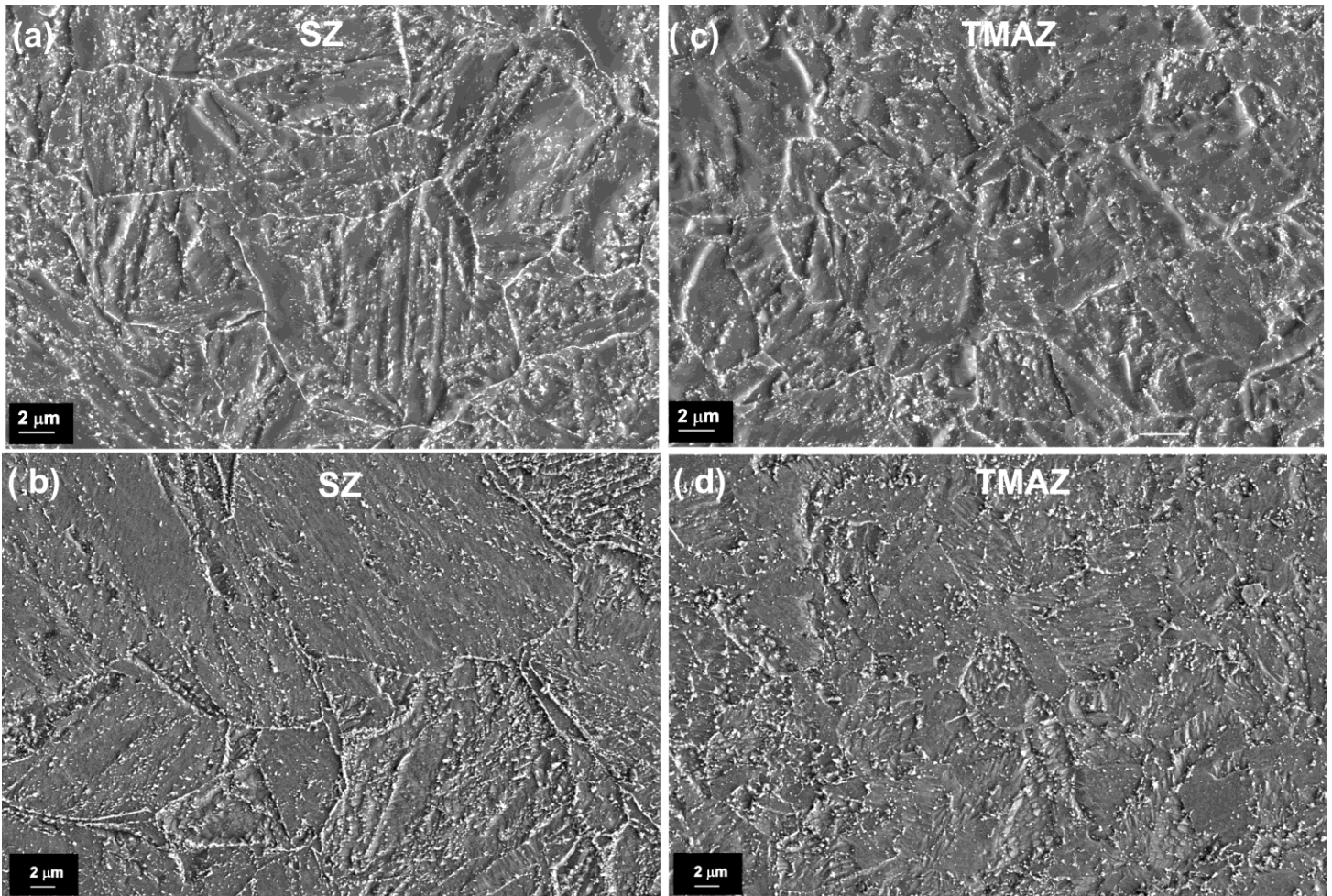


Fig. 6 Vickers hardness profile in transverse section at mid plane for(a) 6 mm plate at 500 rpm and(b)12 mm plate at 500 rpm.



FigFig.7 FE-SEM microstructures of SZ and TMAZ in PWHTed condition (a, b) SZ and (c, d) TMAZ for 6mm and 1212 mm plate at 500 rpm.

maximum temperature reached during FSW dictated the microstructure in different zones. In SZ, rotational speeds at and higher than 300 rpm caused the transformation of  $\alpha$ -Ferrite to austenite during FSW with attendant transformation to martensite during cooling. At 200 rpm no such transformation occurred. At 700 rpm, the maximum temperature attained was above  $Ac_3$  and the carbides that impede grain growth were dissolved resulting in coarse grains in SZ. Coarse grains and martensite have also been seen in 300 and 500 rpm conditions where the maximum temperatures recorded were in between  $Ac_1$  and  $Ac_3$ . The maximum temperature in 200 rpm condition was below  $Ac_1$  and no martensite could be observed and the microstructure contained a few very fine MX type carbides within  $\alpha$  laths. In case of 200 rpm the grain size distribution in SZ was similar to that of BM[7-8]. At all the rotational speeds, the majority of the grain boundaries in SZs were found free from  $M_{23}C_6$ . FSW led to fragmentation of  $M_{23}C_6$  and some fine MX precipitates to a sub-critical size and caused subsequent solid state dissolution in SZs. Surprisingly, all the rotational speeds promoted the formation of needle type  $Fe_3C$  in SZs. FSW process produces significant plastic deformation introducing a large number of vacancies and dislocations in the SZ. The vacancies so generated would cause the accelerated diffusion of interstitial solute atoms promoting  $Fe_3C$  formation.

The SZs depicted high hardness irrespective of rotational speeds Fig.3. A rapid fall in hardness in TMAZ was seen as the distance from the SZ increased and finally attained a small trough in a very narrow HAZ. Higher hardness in SZs at and above 300 rpm appears to result from the combined strengthening effects of martensite and  $Fe_3C$  while fine grain size, the undissolved fine MX precipitates and  $Fe_3C$  contribute to strength at 200 rpm. There has been a gradual reduction in maximum temperature attained as the distance from the SZ increased. The microstructure in TMAZ Fig.4 reveals the presence of very fine grains, and precipitates of  $M_{23}C_6$  and MX both in intra and inter-granular regions. This observation indicates that TMAZ experiences lower temperatures and plastic deformation than in SZ; though the plastic deformation is not high enough to cause fragmentation of carbide particles to sub-critical size and their dissolution but adequate to promote dynamic recrystallization at prevailing temperature as evidenced by fine grain size. The soft narrow HAZ could result due to coarsening of carbides as the temperature seen might be slightly below  $Ac_1$ ; however, the grain size in the HAZ of 6 mm plate remained similar to that in BM.

FSW of 12 mm plate provided some interesting observations compared to the microstructures and hardness obtained on 6 mm plate in different zones. At identical rotational speed of 500 rpm, the heat input was higher in case of 12 mm thick plate Table.2. The width of SZ in 12 mm plate increased and hardness in SZ decreased. The SZ of 12 mm plate showed an average grain size of 18  $\mu m$  against 10  $\mu m$  recorded for 6 mm plate. The SZ exhibited coarse grain martensite and contained  $Fe_3C$  in intragranular regions. The 12 mm plate SZ too revealed carbide-free grain boundaries Fig.5. The microstructure in TMAZ lying close to SZ and

far away from SZ are different. The TMAZ in adjoining regions of SZ displayed fine grain martensite and undissolved carbides during FSW. The fine grain size seems to be associated with continuous dynamic recrystallization. The far TMAZ showed some amount of martensite,  $\alpha$  ferrite and carbides. This observation indicates that the maximum temperature experienced in far TMAZ region is in between  $Ac_3$  and  $Ac_1$ , which is known as intercritical temperature range. The partial amount of austenite formed in this range during FSW gets transformed to martensite during cooling, giving rise to a mixture of martensite,  $\alpha$  ferrite and carbides. In 12 mm plate the HAZ was more prominent and this observation is also reflected in the development of a pronounced dip in hardness Fig.6. It can be noticed from Table-2, in case of 500 rpm, the 12 mm plate requires as much as two times higher heat input than that of 6mm. Hence, the cooling rates are slower in 12 mm thick plate and HAZ was much larger. As mentioned earlier in case of 6mm, the HAZ in 12 mm gets exposed to temperatures below  $Ac_1$ , and therefore the initial BM structure would be subjected to further tempering. The lower hardness could be associated with coarsening of tempered martensite.

### 3.3 Post weld heat treatment

The high hardness in the SZ is detrimental for impact toughness while grain boundaries free from precipitation are prone to grain boundary sliding and inter granular fracture under creep conditions. The presence of needle shaped  $Fe_3C$  in SZ is also undesirable. These undesirable features can be eliminated by appropriate PWHT. Both 6 and 12 mm thick FSW samples were subjected to a PWHT comprising of direct exposure to 760°C/90 min followed by air cooling. The PWHT promoted precipitation of carbides on the grain boundaries as well as in intragranular regions in SZ of both 6 and 12 mm thick plates, as shown in Fig.7(a,b). Additional fine precipitation occurred in TMAZ as revealed in Fig.7(c,d). Microstructure did not reveal the needle shaped  $Fe_3C$

After PWHT, hardness in the SZ was drastically decreased for both 6 and 12 mm thick plates as shown in Fig. 6. In general, 12 mm thick plate welds revealed lower hardness. The hardness in HAZ of 6 mm plate was maintained above 200 VHN, in spite of a small trough in hardness in the HAZ. In case of 12 mm thick welds, the HAZ regions displayed much lower hardness than 200 VHN which is unacceptable for a ferritic-martensitic steel. Such lower hardness regions have been shown to cause pre-mature failures in ferritic-martensitic steels due to the occurrence of Type IV cracking during creep[10]. PWHT led to tempering of the martensite produced in SZ and TMAZ. The pronounced dip in hardness in the HAZ for 12 mm thick weld resulted from coarsening of prior existing precipitates and increase in the lath width. In order to avoid very low hardness in 12 mm thick plate welds, it is recommended that FSW is to be conducted employing low rotational speeds that give rise to low heat input.



#### 4. CONCLUSIONS

1. Full penetration defect free friction stir welds could be successfully produced employing PcBN tools on 6 and 12 mm thick plates.
2. Rotational speed of the tool exerted major influence on the development of heat input and the maximum temperature developed in FSW welds. At identical rotational speeds, higher thickness of plate requires more heat input.
3. The maximum temperature achieved in FSW process was dependent on section thickness. Higher rotational speeds lead to the formation of martensite in SZ and certain times in TMAZ causing very high hardness in these zones.
4. Section thickness strongly influenced the size of SZ, TMAZ and HAZ regions and the overall hardness attained in as-welded state.
5. PWHT was found beneficial in decreasing the hardness of SZ and enabling the desirable precipitation of grain boundary carbides. The excessive softening of HAZ in higher thickness weld results from over tempering of the BM microstructure associated with the coarsening of carbides and dislocation substructure.
6. This study suggests that the ability to produce full penetration welds requires careful consideration and selection of tool material and rotational speed.

#### REFERENCES

- [1] Raj B, Bhanu Sankara Rao K, Bhaduri AK, Progress in the development of reduced activation ferritic martensitic steels and fabrication technologies in India, *Fus Eng. Des.* 85:2010:1460-1468.
- [2] Aubert P, Tavassoli F, Rieth M, Diegele E, Poetivin Y, Review of candidate welding processes of RAFM steels for ITER test blanket modules and DEMO, *J Nuclear Mater* 416: 2011:43-50
- [3] Qingsheng W, Effect of post-weld heat treatment on the mechanical properties of electron beam welded joints for CLAM steel, *J Nucl Mater* 442:2013:512-517
- [4] Shiju S, Das CR, Ramasubbu V, Albert SK, Bhaduri AK, Delta ferrite in the weld metal of reduced activation ferritic martensitic steel, *J Nucl Mater* 455:2014:343-348.
- [5] WeiTang, Jian Chen, Heat input and post weld heat treatment effects on reduced activation ferritic martensitic steel friction stir welds. *Friction stir welding and processing VIII*.
- [6] S. Noh, H. Tanigawa, H. Fujii, A. Kimura, J. Shim, and T. K. Kim: Microstructural evolutions of friction stir welded F82H steel for fusion applications, *Trans. Korean Nucl. Soc. Autumn Meeting, Gyeongju, Korea, October 25-26, 2012*
- [7] Vijaya.L.Manugula, K.V. Rajulapati, G.M. Reddy, R. Mythili and K. Bhanu Sankara Rao: *Mater. Design*, 2016, Vol. 92, pp.200-212.
- [8] Vijaya.L.Manugula, K.V. Rajulapati, G.M. Reddy, E.Rajendra Kumar and K. Bhanu Sankara Rao: *Science and technology of welding & joining*, 2018, Vol. 23.
- [9] Raju S, Jeyaganesh B, Rai AK, Mythili R, Saroja S, Mohandas E, Vijayalakshmi M, Bhanu Sankara Rao K, Raj B, Measurement of transformation temperatures and specific heat capacity of tungsten added reduced activation ferritic–martensitic steel, *J Nucl Mater*, 389:2009:385-393.
- [10] Laha K, Chandravathi KS, Parameswaran P, Bhanu Sankara Rao K and Mannan, Characterisation of microstructures across the heat-affected zone of the modified 9Cr-1Mo weld joint to understand its role in promoting type IV cracking *Metall Mater Trans A* 38A,2007 58-67